# Cyclic Behaviour and Dynamic Properties of Texcoco Clays near Mexico City

Efraín Ovando[1], Zaira Hernández[1], Osvaldo Flores[1], and Alfonso Fernández[1]
[1]*Instituto de Ingeniería, Universidad Nacional Autónoma de México, México City*
*E-mail*: eovs@pumas.ii.unam.mx

**ABSTRACT:** The soft clayey soils of the Former Texcoco Lake, a few kilometres north of Mexico City are highly compressible materials that exhibit very low shear strengths and are also characterized by having extremely high water contents. These soils have been studied extensively in the past but a revision of its properties and characteristics in now in order because large infrastructure works are under way or are being planned to operate in the zone in the near future. This paper presents an overview of some of the results of recent research into the dynamic behaviour of Texcoco Clays carried out at the National University of Mexico. We present the results of one way consolidated-undrained cyclic triaxial tests in which we varied cyclic amplitude as well applied stresses using high quality samples retrieved from the site. Results are also expressed in terms of accumulated strains and in terms of the evolution of pore pressure during cyclic loading. We complement the results of these tests with those obtained from torsional resonant column tests in which we assess an analytical model to express the stiffness-strain and damping-strain characteristics of these materials. We also look at the relationship of small strain stiffnesses obtained in resonant column tests and those found from the results of bender element measurements and from the results of field measurements using the suspension logging technique. We also put forth correlations between the dynamic parameters obtained in the lab and in the field with data from CPT tests. Finally, we discuss the significance of these tests bearing in mind that the site is subjected to regional subsidence due to the exploitation of the aquifers that underlie the clayey strata.

**KEYWORDS:** Cyclic behavior of soft clays, Properties of Texcoco clays, México City, Test on cyclic triaxial cells and resonant column.

## 1. INTRODUCTION

In this paper, we look at some of the results of dynamic tests performed on clay samples retrieved from a site some 15 km north of Mexico City that was formerly occupied by the Texcoco Lake. This water body formed part of a rather big lake system in the Mexico Basin which comprised six great lakes: Ecatepec, Zumpango, Texcoco, Mexico, Xochimilco and Chalco, which were formed in the Upper Quaternary after the Sierra Chichinautzin closed the watershed of the Basin of Mexico in its southern border. The static properties of the soils in Lake zone of Mexico City have been extensively studied by Marsal and Mazari (1959), Carrillo (1969), Giraldo and Ovando-Shelley (1996), Alanís (2003), Ovando-Shelley et al. (2007) and Ovando-Shelley (2011), among others. Other studies have focused on the dynamic properties of the Mexico City clays by means of laboratory tests (Romo et al., 1988; Romo, 1995; Romo and Ovando, 1996). Field measurements of the shear wave velocity have been performed using suspension conventional geophysical methods (cross-hole, down-hole, PS logging), as well as estimations from the results of CPT tests (Ovando-Shelley and Sámano, 1993). It has also been shown that regional consolidation induced by water pumping in the lake zone increases effective stresses in the subsoil which, in turn, modify static and dynamic soil properties (Ovando-Shelley et al., 2007). These changes have modified the characteristic of seismic response at the site.

The geotechnical knowledge gained throughout time has allowed engineers in the city to face projects with an improved understanding of the difficulties that must be met in any kind of construction. Still, there are many aspects of the behavior of the lacustrine Mexico City Clays that require further research, especially those located in what used to be the former Texcoco Lake, located in the northern portion of the Greater Mexico City urban area. In this respect, concerns regarding the dynamic properties of these materials must be addressed, given that the zone is very active seismically. In what follows, we summarize some of the main findings of an extensive testing program that was carried out in connection to the construction of a new airport for Mexico City in the former Texcoco Lake.

## 2. GENERAL GEOTECHNICAL ENVIRONMENT

Lake Texcoco used to be the largest body of water in the northern portion of the Basin of Mexico. The graph in Figure 1 provides a sketch indicating the position of the former Lake Texcoco with respect to Mexico City and other adjoining states. Up until the turn of the century, this zone had never been subjected to external overburdens. Nonetheless, the zone was subjected to the effects of very intense shallow pumping in the western portion for the production of caustic soda, an operation that ended in the 1970s. Deep well pumping for the exploitation of the aquifers that underlie the lacustrine soils is an ongoing operation for more than 50 years. It has been estimated that local and regional pumping has induced total settlements in the zone of more than 8 m over a 20 year period (Ovando et al., 2007).

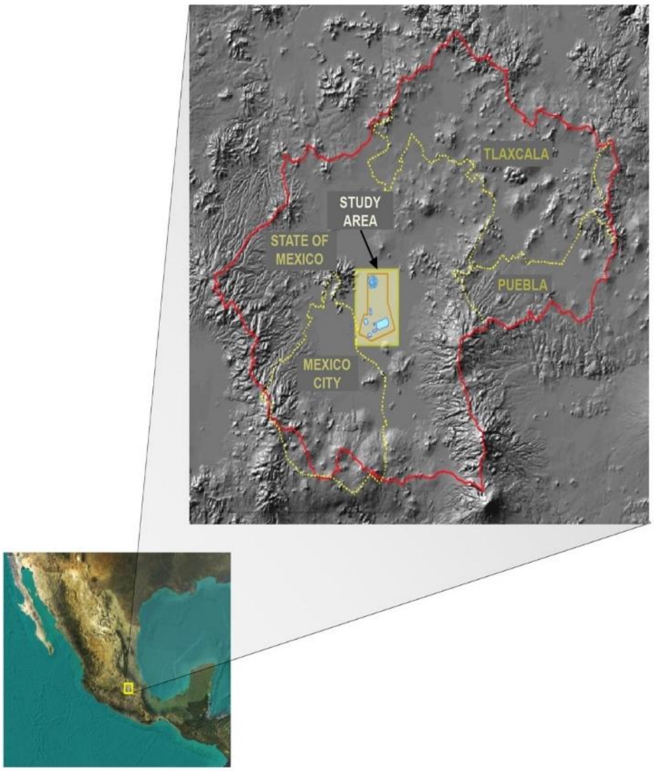

Figure 1 Location of the Texcoco Lake area

As seen in Figure 2, the subsoil is constituted by three potent layers of lacustrine soft clay interspersed with layers and lenses of other harder more permeable materials, as follows:

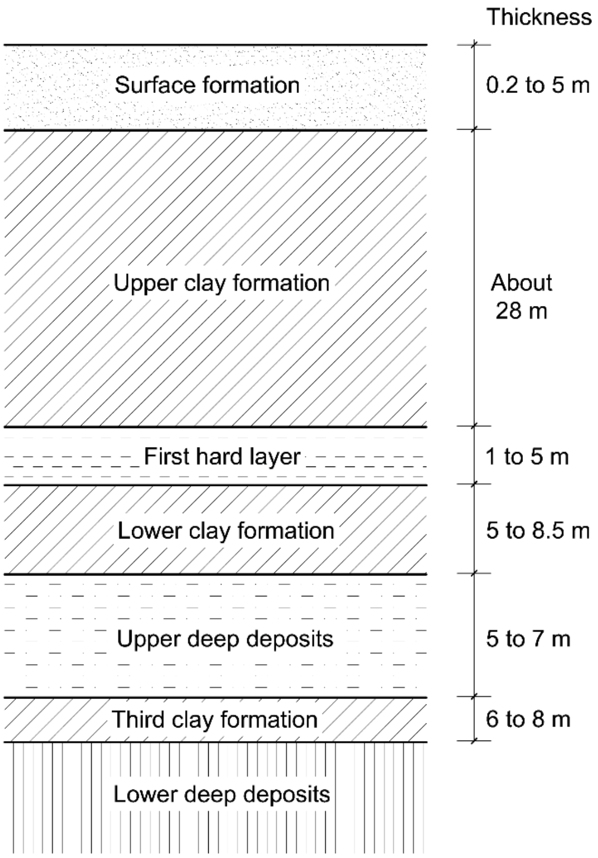

Figure 2 Simplified stratigraphy at the former Texcoco Lake taken from Flores et al. (2014)

- *Surface formation*: It is a sun-dried layer formed with silty clays and silty sands, 0.2 to 5.0 m thick. It is thicker towards the northeast of the federal zone and is rather thin in its southwest portion. CPT strength varies between 0.5 and 10 MPa, with the lower strengths in the southwest and the highest towards the northeast; corresponding water contents vary from 50 to 75%. The uppermost materials in this formation are fissured vertically due to seasonal drying and wetting. Fissures are often in-filled with wind driven soils. Phreatic water is found within this formation and it seldom deeper than about 1 m.
- *Upper clay formation*: This is a potent stratum of high plasticity lacustrine clay that may be as much as 28 m thick towards the central part of the former lake area and around 10 m near its edges; thin lenses and layers of coarser alluvial soils are often found interspersed with the clays. The uppermost materials are slightly preconsolidated due to solar drying. This formation contains the materials having the largest water contents which average 250% but may even exceed 600%. CPT strength may vary between 0.1 to 0.5 MPa and may be as high as 0.8 MPa in the harder materials found near the transitional zones at the edges of the former lake.
- *First hard layer*: It's a sequence of sandy and lightly cemented silty soils, interspersed with soft clayey soils that may at times be represented by one single stratum. This stratum appears at variable depths, from about 12 m to more than 29 m and its thickness can vary from 1.5 to 5 m and its water content from 20 to about 70%. CPT strengths are usually larger than 10 MPa and SPT penetration resistance can often exceed 50 blows.
- *Lower clay formation*: It has the same origin and roughly the same characteristics as the upper clays albeit water contents in these clays are lower and are less compressible with correspondingly higher shear strengths. CPT strengths vary between 0.5 and 1 MPa, its thickness from 5 to 8.5 m. It is also interspersed with thin lenses of sandy silts where CPT strength may be larger than 10 MPa. These harder lenses are more abundant than in the upper clay formation.
- *Upper deep deposits*: These form the so called second hard layer and are found at about 40 m from the surface and are 5 to 7 m thick. They contain silts as well as very compact fine silty sands. These materials display rather large penetration resistance: more than 100 blows in SPT tests. The water content range spans from 15 to 63%.
- *Third clay formation*: These are slightly more consistent than the clays in the lower clay formation, despite appearing at considerable larger depth, typically in excess of 42 m with thicknesses varying between 6 and slightly less than 8 m.
- *Lower deep deposits*: The materials present in these deposits are very compact and partly cemented sands and silty sands, with water contents that seldom exceed 30%. They appear at depths of sligltly more than 50 m and continue down to about 100 m. Other compressible strata can also be found at larger depths (Marsal and Graue, 1969).

## 3. TESTING PROGRAM

In regard to the project for a new airport for Mexico City in the former Texcoco Lake over an area of 4,431 Ha, a large number of tests were carried out in order to characterize its subsoil in the most detailed manner that was technically and economically feasible. In this document, we discuss the results of some of these tests that include cyclic triaxial tests, resonant column (Drnevich type) and conventional consolidated undrained tests in which seismic wave velocities were measured with piezo electric crystals.

## 4. TESTING BEHAVIOUR OF TEXCOCO CLAY UNDER ONE WAY CYCLIC LOADING

A series of one way cyclic triaxial tests was performed on samples retrieved from the Upper Clay Formation. An example of the results obtained is given in the following paragraphs by looking at the results of tests performed on three samples retrieved from the Upper Clay Formation having different index properties, as indicated in Table 1. Each sample was subjected to 100 sinusoidal load cycles with a period of 1.0 s. After the application of the load trains, the drainage line was opened to dissipate excess pore pressure generated during cyclic loading. Upon the reconsolidation of the specimen, a new train of undrained cyclic loads was then applied.

Table 1 Index properties of samples tested with different qcyc/qf ratios (Figures 3 to 6)

| **Borehole** | **Sample** | **Depth (m)** | **w (%)** | **e** | **PI (%)** | **$G_s$** |
|---|---|---|---|---|---|---|
| SS-01 | 4 | 14.90 | 223.37 | 7.80 | 207.63 | 3.45 |
| SM-20 | 27 | 13.05 | 173.37 | 5.34 | 131.03 | 3.09 |
| SS-03 | 2 | 6.40 | 292.60 | 9.73 | 232.53 | 3.34 |

The graphs in Figure 3 show typical stress-strain hysteresis loops obtained from tests performed on one of these samples. The figure shows the loops obtained from the first loading cycle. Cyclic stress amplitudes indicated in the figure are expressed as fractions of the static shear strength, $q_{cyc}/q_f$. In looking at the hysteresis loops, stiffness degradation is evident as cyclic stress amplitudes increase. Note that for a cyclic stress amplitude $q_{cyc}/q_f = 1.0$, the sample did not fail, albeit straining reached a relatively large magnitude of slightly more than 3%; failure in this sample was reached on cycle 68.

Accumulation of excess pore pressure with cyclic loading turned out to be rather modest and, as seen in Figure 4, most of the excess pore pressure was generated during the first cycle. For the larger amplitude, $q_{cyc}/q_f = 1.0$, excess pore pressure normalized with respect to the confining pressure only attained the value of $\Delta u/\sigma'_c = 0.4$ but, as indicated previously, this specimen failed abruptly after 68 cycles. It is also interesting to note that $\Delta u/\sigma'_c$ varies linearly with $q_{cyc}/q_f$, for N < 50, as shown in Figure 5.

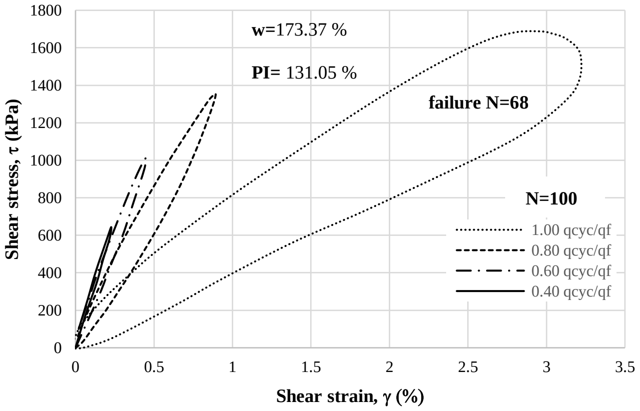

Figure 3 Typical hysteresis loops obtained from a one way cyclic triaxial test on a sample of Texcoco Clay

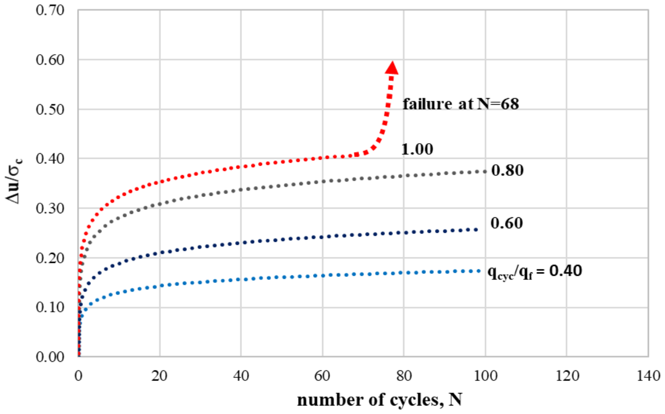

Figure 4 Typical hysteresis loops obtained from a one way cyclic triaxial test on a sample of Texcoco Clay

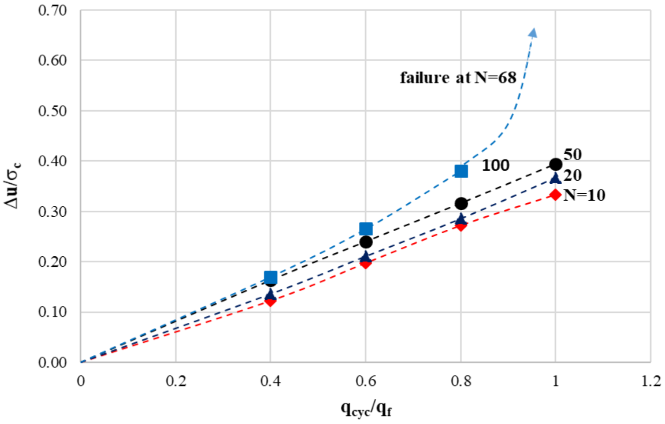

Figure 5 Excess pore pressure generated after specific load cycles, as functions of cyclic stress amplitude

Shear modulus degradation of the three samples is illustrated in Figure 6 in which the value of shear modulus, G, was plotted against the normalized cyclic stress amplitude, $q_{cyc}/q_f$. Data from resonant column tests is also plotted for samples SM-20 and SS-03 (see Table 1). In general G remains nearly constant up $q_{cyc}/q_f$ values of about 0.5. Thereafter G decreases linearly as the cyclic stress amplitude increases. Note that cyclic stress amplitudes may exceed static shear strength, a situation that had been noted previously by other researchers in the past (Romo et al., 1988; Romo and Ovando, 1996).

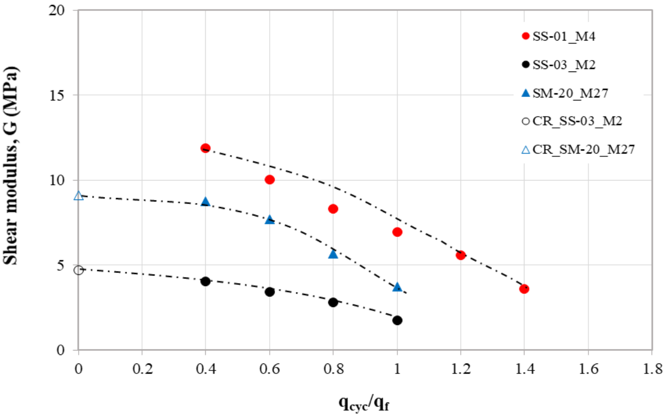

Figure 6 Shear modulus as a function of cyclic stress amplitudes

## 5. MODIFIED TEXCOCO CLAY MODEL (MTCM)

Researchers have recognized that highly plastic clays behave as nearly elastic materials over the small strain range (Dobry and Vucetic, 1991; Romo and Ovando, 1996). In clays having very large plasticity indexes, the strain range over which linear pseudo elastic behavior is much larger than for the lower plasticity materials. As part of the research for the Texcoco Airport Project it was necessary to develop an *ad hoc* stiffness degradation model and in it, soil plasticity is incorporated explicitly. The model was derived from a parametric analysis performed using Davidenkov´s model and experimental data from resonant column and cyclic triaxial tests. The equations presented here modify those presented previously by González and Romo (2011). The Modified Texcoco Clay Model (MTCM) is defined by means of the following equations:

$$G = (G_{mín} - G_{máx})H_G + G_{máx} \tag{1}$$

$$\lambda = (\lambda_{máx} - \lambda_{mín})H_\lambda + \lambda_{mín} \tag{2}$$

$$H_G = \frac{\left(\frac{\gamma}{\gamma_{rG}}\right)^{2B_G}}{1+\left(\frac{\gamma}{\gamma_{rG}}\right)^{2B_G}} \tag{3}$$

$$H_\lambda = \frac{\left(\frac{\gamma}{\gamma_{r\lambda}}\right)^{2B_\lambda}}{1+\left(\frac{\gamma}{\gamma_{r\lambda}}\right)^{2B_\lambda}} \tag{4}$$

where $G_{máx}$ and $\lambda_{mín}$ are the values of shear modulus, G, and damping ratio, λ, for the range of strains in which the soil behaves elastically; $G_{mín}$ and $\lambda_{max}$ are the values of G and λ before the soil reaches failure under dynamic loads; $\gamma_{rG}$ and $\gamma_{r\lambda}$ are reference strains corresponding to the inflection points in experimental G-γ and λ-γ curves (see Figure 7); $B_G$ y $B_\lambda$ are experimentally derived constants that define the geometry of G-γ and λ-γ curves (see Figure 8).

$G_{máx}/\sigma'_c$ may be obtained as a function of the plasticity index by means of the following empirical correlation that was derived from test data presented in Figure 9.

$$\frac{G_{máx}}{\sigma'_c} = 30905\ IP^{-1.138} \tag{5}$$

Reference strains $\gamma_{rG}$ and $\gamma_{r\lambda}$ as well as the constants $B_G$ y $B_\lambda$, are also determined from the following are additional set of empirical correlations, also expressed in terms of IP, the plasticity index.

$$\gamma_{rG} = 2e^{-5}\ IP^{2.0209} \tag{6}$$

$$\gamma_{r\lambda} = 0.0048\ IP + 0.0583 \tag{7}$$

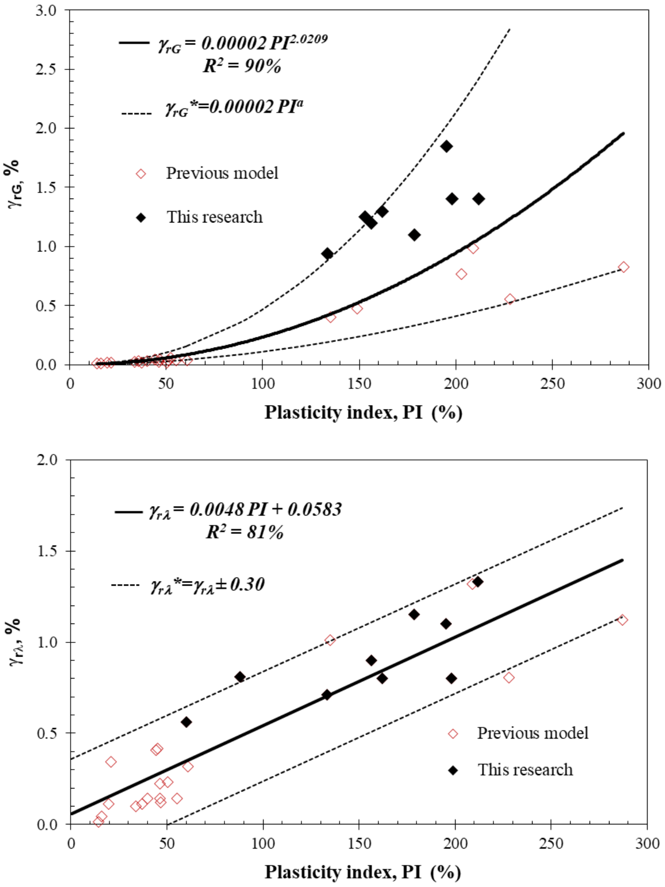

Figure 7 Normalized value of maximum shear modulus in terms of plasticity index

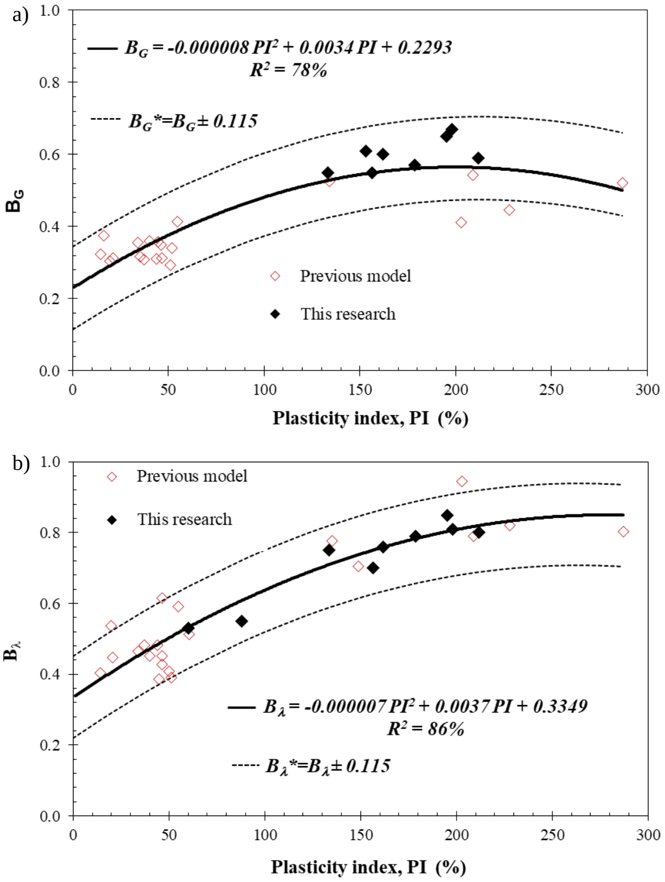

Figure 8 (a) Normalized Experimentally derived constants BG and (b) Bλ, as a function of plasticity index

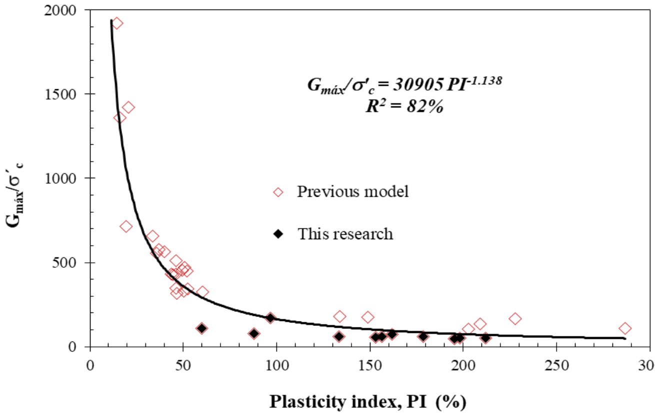

Figure 9 Normalized value of maximum shear modulus in terms of plasticity index

$$B_G = -8e^{-6}\, IP^2 + 0.0034\, IP + 0.2293 \qquad (8)$$

$$B_\lambda = -7e^{-6}\, IP^2 + 0.0037\, IP + 0.3349 \qquad (9)$$

The graphs in Figure 10 present a set of G/G$_{max}$ -γ and λ-γ curves obtained experimentally, compared with curves plotted using the empirical MTCM. As seen, our model provides a very good approximation to the actual curves and it was used. The MTCM is not to be generalized since it was obtained from correlations valid only for the Texcoco Clays studied in this research.

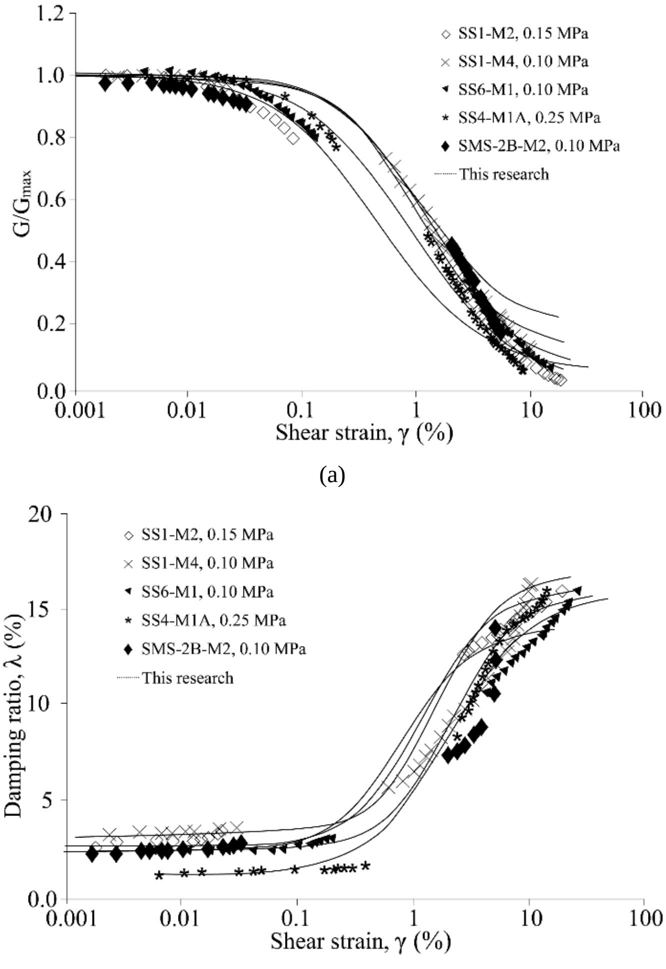

(a)

(b)

Figure 10 (a) G/G$_{max}$ vs. γ and (b) damping ratio vs. γ curves. Full lines are curves calculated with the MTCM; data points obtained from the tests on lacustrine specimens

Table 2 Index properties of the specimens tested to calibrate the MTCM (Figure 9)

| Borehole | Sample | Depth (m) | w (%) | e | PI (%) | $G_s$ |
|---|---|---|---|---|---|---|
| SS-1 | 2 | 4.85 | 252.97 | 6.68 | 156.33 | 2.58 |
| | 4 | 15.85 | 244.87 | 7.42 | 211.81 | 3.03 |
| | 7 | 39.95 | 132.28 | 3.52 | 133.41 | 2.71 |
| SS-6 | 1 | 4.45 | 255.24 | 6.42 | 178.63 | 2.49 |
| SS-4 | 4A | 26.30 | 247.30 | 6.36 | 195.27 | 3.24 |
| | 6A | 56.70 | 91.81 | 2.57 | 88.03 | 2.65 |
| SMS-2B | 2 | 13.40 | 231.54 | 7.67 | 153.22 | 3.21 |
| SS-03 | 6 | 25.70 | 195.70 | 6.61 | 198.19 | 3.34 |

## 6. SEISMIC WAVE VELOCITIES FROM FIELD AND LABORATORY TESTS

Experiments on Texcoco Clay also included tests on samples tested in triaxial cells provided with piezoelectric crystals to measure seismic compression and shear wave velocities, $V_p$ and $V_s$, respectively. Techniques to interpret signals produced by compression and bender piezoelectric elements have been discussed amply by many researchers in the past (Styler and Howie, 2014; Yamashita et al., 2009). The technique is now used routinely in many laboratories and can be adapted to various testing devices (Shibuya, 2005). Regarding the Texcoco Clays, Flores-Guzmán et al. (2014) demonstrated produced useful data to characterize these materials by means seismic wave velocities measured in a triaxial cell provided with piezoelectric crystals.

Field tests were also carried out at a particular site to measure seismic wave velocities using three different techniques. One of them was the so called seismic Marchetti dilatometer which is essentially the original Marchetti probe equipped with geophones to record inside the soil the arrival of waves generated at the surface, i.e. this gear provides a means of performing typical down-hole tests. Seismic wave velocities were also measured using the well-known cross-hole technique and the suspension logging technique originally developed by Oyo Corporation and described in detail by Biringen and Davie (2010).

The graph in Figure 11 shows the values of shear wave velocity determined from the three field techniques described previously, plotted against depth. As seen in the graph, shear velocities obtained from the cross-hole test turned out to be quite larger than those obtained with the seismic Marchetti device, especially over the 5 to 12 m depth range. The reasons for these discrepancies certainly require more investigation but it can tentatively be assumed that travel paths and soil anisotropy may certainly influence the results. Travel paths in the cross hole test are essentially horizontal and shearing is generated along vertical planes whereas in the down-hole technique (seismic Marchetti probe) seismic waves travel along inclined paths from the source down to the receiving geophone. Shear waves are mostly perpendicular to the path travelled by the waves. In both cases waves may diffract and refract, when passing through materials having contrastingly different densities, a situation that will produce noise in the recorded signals, a situation that can difficult their interpretation. Values obtained with the suspension logging technique fall exactly in between the values obtained with the other two techniques in the shallower depths.

Shear wave velocities obtained from bender element measurements and from resonant column tests at small strains, tend to lie close to the values obtained with the suspension logging technique. There values of shear wave velocities obtained from resonant column tests that are considerably higher than any of the other values obtained from either field or laboratory measurements. These were in general obtained from specimens lower plasticity indexes and in which inclusions or seams of non-plastic materials were found.

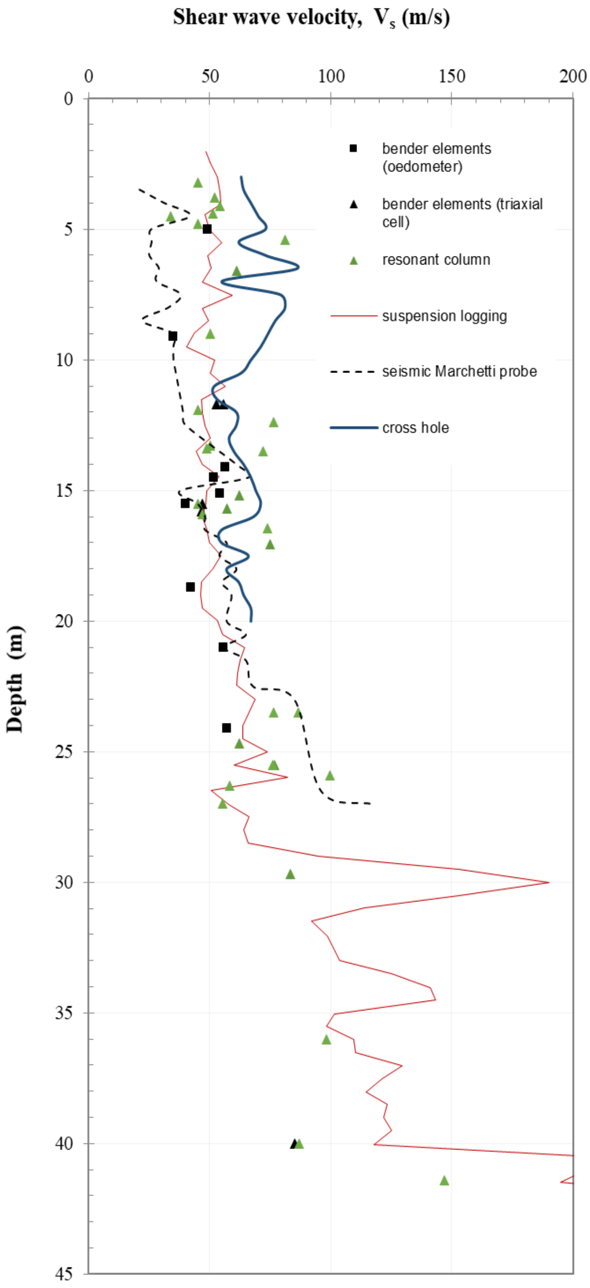

Figure 11 Shear wave velocity profiles obtained with three different field techniques. Data from resonant column tests and bender element measurements also included

## 7. CONCLUSIONS

This paper presented an example of typical cyclic triaxial test results performed in Texcoco Clay specimens. Results presented here form part of a rather broad field and laboratory investigation performed for the project for the new Mexico City Airport in the former Texcoco lake. Results confirm, in general, other observations made previously in regard to the behavior of these materials under cyclic loading:

- Stiffness, i.e. shear modulus values at small cyclic stress amplitudes are associated with small values of hysteretic damping values.
- Shear modulus remains nearly constant up cyclic stress amplitudes of about $q_{cyc}/q_f = 0.5$. For larger cyclic stress ratios, shear moduli decreased linearly.
- There were cases in which $q_{cyc}/q_f > 1.0$, i.e. when cyclic stress amplitude exceeded static shear strength, a situation that had been noted previously (Jaime, 1988; Romo and Ovando, 1996).

All these observations are consistent with the notion that Texcoco Clays behave as vicous-elasto-plastic solids.

The paper presented a stiffness-damping-strain model, the Modified Texcoco Clay Model (MTCM) that provides can very closely reproduce the behaviour of these clays under dynamic loading and that was used in site response analyses and in soil-structure interaction studies for a large project that was planned in the former Texcoco Lake. The MTCM is based on the Davidenkov model and was calibrated with test data performed in Texcoco Clays. Hence, it cannot be generalized for other materials.

## 8. REFERENCES

Alanís González, R. (2003) “Caracterización geotécnica del ex–lago de Texcoco”, MSc Thesis, School of Engineering, Universidad Nacional Autónoma de México.

Biringen, E., and Davie, J. (2010) “Suspension P-S Logging for Geophysical Investigation of Deep Soil and Bedrock”, Advances in Analysis, Modeling & Design IEC S. C., (2014).

Carrillo, N. (1969) “The subsidence of Mexico City and Texcoco Lake”, Texcoco Project.

Fores-Guzmán, M., Ovando-Shelley, E., and Valle-Molina, C. (2014) “Small strain dynamic characterization of clayey soil from the Texcoco Lake, Mexico”, Soil dynamics and Earthquake Engineering, 63, pp1-7.

Giraldo S. M., and Ovando Shelley, E. (1996) “Evaluación de un modelo elasto-plástico para predecir el comportamiento de la arcilla de la ciudad de México”, Engineering Institute, Universidad Nacional Autónoma de México.

González, C. M., and Romo, M. P. (2011) “Estimación de propiedades dinámicas de arcillas, Revista de Ingeniería Sísmica”, México, No. 84, pp1-23.

Marsal, R., and Mazari, M. (1959) “The subsoil of Mexico City”, Mexico City, Facultad de Ingeniería, UNAM.

Marsal, R. J., and Graue, R. (1969) “El subsuelo del lago Texcoco”, Volumen Nabor Carrillo, Ministry of Finance and Public Credit, Mexico, pp167-202.

Ovando, E., and Samano, A. (1993) “Ensayes de cono sísmico en la Ciudad de México”, Engineering Institute, Universidad Nacional Autónoma de México.

Ovando, E., Ossa, A., and Romo, M.P. (2007) “The sinking of Mexico City: its effect on soil properties and seismic response”, Inte J Soil Dyn Earthquake Engineering, 27, pp333-343.

Ovando-Shelley, E. (2011) “Some geotechnical properties to characterize Mexico City Clay”, Proceedings of the 14th Panamerican conference of soil mechanics and geotechnical engineering”, Paper 889, Canadian Geotechnical society.

Romo, M.P0, Jaime, A., and Reséndiz, D. (1988) “General soil conditions and clay properties in the Valley of Mexico”, J Earthquake SPECTRA 1988, 4(2), pp731–752.

Romo, M.P. (1995) “Clay behavior, soil response and soil structure interaction studies in Mexico City”, Proceedings of the third international conference on recent advances in geotechnical earthquake engineering and soil dynamics, San Luis Missouri, USA, vol. 2, pp1039-1051.

Romo, M.P., and Ovando, E. (1996) “Modelling the dynamic behaviour of Mexican Clays”, Proc. 11 World Conference on Earthquake Engineering, Acapulco, Mexico.

Shibuya, S., Koseki J., and Kawaguchi, T. (2005) “Recent developments in deformation and strength testing of geomaterials”, Deformation Characteristics of Geomaterials, Recent Investigations and Prospects, Di Benedetto, et al. Eds., Taylor and Francis Group, London, 1, pp3-29.

Styler, M., and Howie, J. (2014). “Continuous monitoring of bender element shear wave velocities during triaxial testing”, Geotechnical Testing Journal, 37, pp218-229.

Yamashita, S., Kawaguchi, T., Nakata, Y., Mikami, T., Fujiwara, T. and Shibuya, S. (2009) “Interpretation of international parallel test on the measurement of Gmax using bender elements”, Soils and Foundations, 49, pp631-650.